IOPscience iopscience.iop.org

Home Search Collections Journals About Contact us My IOPscience

A constrained-equilibrium Monte Carlo method for quantum dots—the problem of intermixing

This article has been downloaded from IOPscience. Please scroll down to see the full text article.

2004 J. Phys.: Condens. Matter 16 S1485

(http://iopscience.iop.org/0953-8984/16/17/004)

View the table of contents for this issue, or go to the journal homepage for more

Download details:
IP Address: 129.252.86.83
The article was downloaded on 27/05/2010 at 14:29

Please note that terms and conditions apply.

INSTITUTE OF PHYSICS PUBLISHING JOURNAL OF PHYSICS: CONDENSED MATTER

J. Phys.: Condens. Matter **16** (2004) S1485–S1501 PII: S0953-8984(04)66671-9

A constrained-equilibrium Monte Carlo method for quantum dots—the problem of intermixing

P C Kelires

Physics Department, University of Crete, PO Box 2208, 710 03 Heraclion, Crete, Greece
and
Foundation for Research and Technology–Hellas (FORTH), PO Box 1527, 711 10 Heraclion, Crete, Greece

Received 23 July 2003
Published 16 April 2004
Online at stacks.iop.org/JPhysCM/16/S1485
DOI: 10.1088/0953-8984/16/17/004

Abstract

Islands grown during semiconductor heteroepitaxy are in a thermodynamically metastable state. Experiments show that diffusion at the surface region, including the *interior* of the islands, is fast enough to establish local equilibrium. I review here applications of a Monte Carlo method which takes advantage of the quasi-equilibrium nature of quantum dots and is able to address the issue of intermixing and island composition. Both Ge islands grown on the bare Si(100) surface and C-induced Ge islands grown on Si(100) precovered with C are discussed. In the bare case, the interlinking of the stress field with the composition is revealed. Both are strongly inhomogeneous. In the C-induced case, the interplay of strain and chemical effects is the dominant key factor. Islands do not contain C under any conditions of coverage and temperature.

(Some figures in this article are in colour only in the electronic version)

1. Introduction

The transition from a planar, layer-by-layer two-dimensional (2D) growth mode to a 3D mode during semiconductor heteroepitaxy, characterized by the formation of nanometre-scale islands, has been the subject of intensive studies during the last decade. These islands, usually referred to as quantum dots (QDs), are of great fundamental and technological interest. Much of the latter stems from their property of localizing and strongly confining the carriers spatially in three dimensions, which makes them promising candidates for use in optically active devices with strong photoemission signals.

It has become apparent that the most challenging problem for a complete description of the islanding phenomenon is the issue of *intermixing*. Without analysing and settling this issue, many other important processes cannot be fully understood. These include the island nucleation process [1–3], self-assembling and organization [4], and shape transitions [5]. For example, significant interdiffusion and mixing of species is expected to affect the nucleation process, because the strain field due to the mismatch will be unavoidably altered and any

strain-driven mechanism has to take this into account. For surface kinetic processes we also need to consider the effect. Similar arguments apply in the case of shape transitions occurring either after post-growth thermal annealing or during capping of the dots with the host material.

But most importantly, intermixing and its extent are expected to affect the confinement within the QDs and their optoelectronic properties. It is therefore vital to gain knowledge about the composition variations within the islands. Note that not only is mere mixing of species an important factor, but so also are any variations of composition and the resulting inhomogeneities. Another related issue is the interlinking of interdiffusion with the stress field in the system. While there have been in the past numerous theoretical investigations of the stress field in QDs [2, 6–9], no attempts to link stress and composition had been made.

Generally speaking, intermixing is a complicated phenomenon. Simple arguments suggest that interdiffusion of species is favoured, provided that kinetic barriers are overcome, because it lowers the effective lattice mismatch and thus reduces the elastic strain (which partially remains even after islanding takes place). However, whether this phenomenon takes place during or after growth, or at both times, cannot be easily answered. Naturally, higher growth or annealing temperatures would provide the necessary energy to overcome the potential barriers, so a certain degree of intermixing in such cases should be expected. Also, what cannot be speculated beforehand is how compositions vary within the islands and as a function of temperature and size.

From the theoretical point of view, a significant contribution to the problem has been made by Tersoff [10, 11] within continuum elasticity theory. The basic assumption involved in this work is that the composition is determined solely by the variation in strain across the growing island surface, and that there is negligible bulk diffusion within the island. Thus, when the equilibrium surface composition is buried by further growth, it becomes the composition of the interior. However, recent experiments [12] suggesting the possibility for bulk diffusion in the islands shed doubt on this simplification of the problem. We shall discuss this issue in detail in the following section.

Experimentally, a number of studies have addressed the problem [13–19] and suggested that intermixing takes place, but its degree and the stage at which this happens remain controversial. Some of these studies [18, 19] suggested that intermixing is already taking place during growth, especially at high temperatures, *albeit* without quantifying its extent. Other studies [13–15] provided firm evidence that intermixing at medium growth temperatures is rather initiated after island nucleation, and showed that this is possible at even higher temperatures by controlling the deposition rate. Recent experiments [20, 21] made an attempt to probe the composition profiles within Ge/Si(100) islands.

Here, I review recent work [22, 23] carried out in our group, proposing the first direct simulational approach to the intermixing problem. This approach is based on a *quasi-equilibrium* or *constrained* Monte Carlo method. The reasoning for using such a method and its fundamentals will be discussed in the next section. We first applied this methodology to Ge islands formed on Si(100), and I shall only describe here simulations of such dots. We discuss two cases: Ge dots on the *bare* Si(100) surface, and *C-induced* Ge dots, i.e., Ge dots nucleated on Si(100) precovered with small amounts of C. In the latter case, we have the unique opportunity to study the interplay between strain and chemical effects.

2. Methodology

2.1. Physical considerations for equilibrium

The use of the Monte Carlo (MC) method to tackle the problem of intermixing in QDs requires some justification. MC simulation is by definition a method for the equilibrium state.

The key question to be asked, therefore, is whether QDs are in a state of equilibrium. The crucial parameter, able to give an answer to this question, is the extent of diffusion in the near-surface region and within the islands. One point of view is that bulk diffusion in the dots is extremely limited and there is only need to consider surface diffusion events. For example, in the case of interest here, it is frequently argued that deposited Ge atoms, or Si atoms from the already alloyed wetting layer (WL), move freely on the surface and attach at the island edges and facets as the island grows. It is thus assumed that only the surface of the dot is in equilibrium—where the diffusion is fast—and not its interior. So, when further material is deposited on top, the composition in the interior freezes due to the lack of diffusion.

However, recent experiments by the group of Grützmacher [12] gave clear evidence that when Ge dots are subsequently capped with Si at $\sim$800 K, not only is diffusion of the covering material along the facets of the islands taking place, but also significant diffusion of Si atoms from the top towards the centre of the dot, i.e., within its bulk, occurs. This finding is very important because it shows bulk diffusion in the capped dots, and thus implies conditions at least near equilibrium. Note that the capped islands were already intermixed to a certain degree before capping, since the growth temperature was $\sim$900 K, and so they had largely relaxed the internal stress. We can, therefore, safely conclude that diffusion in the growing (uncapped) islands is *even faster* because it is enhanced by the significantly higher strain. Indications for bulk diffusion in the islands are also provided by earlier work [15]. These authors showed that SiGe alloyed pyramids form via Si interdiffusion into pure Ge pyramids.

Given these remarks, we may answer the question posed above as follows: thermodynamically, islands are in a *metastable* phase because diffusion in the surface region, including the island, the WL, and a few monolayers in the substrate is fast due to the strain. Medium and high growth temperatures help to overcome the diffusion barriers and make the effect stronger. As a result of the enhanced diffusion, *local equilibrium* is established, and this means metastability. Of course, the true thermodynamic equilibrium state of the Ge/Si system would be a dilute GeSi alloy, with Ge atoms dissolved deep in the Si bulk but, in practice, the system never reaches this state due to the slow diffusion in the bulk of the substrate. So, what is needed to model the situation is a *quasi-equilibrium* or *constrained-equilibrium* approach, in the sense that it constrains us to sample over the local equilibria of the various metastable phases of the Ge/Si system in the surface region, as defined above. This leads to the following MC algorithms.

2.2. MC algorithms

The statistical ensemble underlying the simulations is, in general, the semigrand canonical (SGC) ensemble. For the bare Ge/Si case, the ensemble is simplified to treat a constant-composition system. For the C-induced dot case, a *biased* MC algorithm is used, devised earlier by the author to deal with C incorporation in the Si, Ge, and SiGe lattices, or with any case where large size mismatch exists between the constituent atoms [24–26].

In the SGC ensemble, denoted as $(\Delta\mu, N, P, T)$, one requires that the total number of atoms N, the pressure P, the temperature T, and the chemical potential differences $\Delta\mu$ remain fixed. These conditions allow fluctuations Δn in the number of atoms of each species, as a result of exchanges of particles within the system, which are driven by the appropriate chemical potential differences $\Delta\mu$ $(=\mu_i - \mu_j,\ i, j \equiv$ Si, Ge, C in the present general case). At the same time, we have also exchanges of volume with the heat bath, as well as the traditional MC moves involving random atomic displacements. Thus, the SGC ensemble can be considered as a combination of the grand canonical (GC) and the more familiar isobaric–isothermal (N, P, T) ensemble. It can be shown that the SGC ensemble is obtained from the GC ensemble upon

imposing the constraint that $N = \sum_i N_i$ is fixed and changing to constant pressure [27]. The resulting partition function (only the configurational part) for an n-component mixture, which couples volume changes and atom-identity flips, is given by

$$Q_{\rm semi} = \beta P \int {\rm d}V\, {\rm e}^{-\beta P V} \frac{V^N}{N!} \sum_{\rm identities} \prod_{i=1}^{n} \left(\frac{\lambda_i}{\lambda_1}\right)^{N_i} \int {\rm d}s^N\, {\rm e}^{-\beta U(s^N)}, \tag{1}$$

where $\lambda_i = {\rm e}^{\mu_i/k_{\rm B}T}$ are the fugacities in the system, $U(s^N)$ is the potential energy associated with both atom identities and displacements, and is a function of the $3N$ scaled atomic coordinates s, and $i = 1$ is the arbitrarily fixed identity to which all chemical potential differences (there are $n - 1$ independent fugacities in the system) are referred. For a detailed derivation of equation (1) see [27].

The implementation of this ensemble for MC simulations is done through the Metropolis algorithm [28], in the following way: the traditional random atomic moves ($s^N \rightarrow s'^N$), leading to a change in the potential energy $U \rightarrow U'$, and the volume changes $V \rightarrow V'$ are accepted with a probability

$$P_{\rm acc} \sim {\rm e}^{-\Delta W/k_{\rm B}T} = \min[1, \exp(-\beta\,\Delta W)], \tag{2}$$

$$\Delta W = (U' - U) + P(V' - V) - Nk_{\rm B}T \ln(V'/V), \tag{3}$$

as in the (N, P, T) ensemble. For the trial moves which select one of the N particles at random, and with equal probability change its identity into one of the other possible identities of the system, the acceptance probability is given by

$$P_{\rm acc}^{\rm iden}(i \rightarrow i') = \min\left[1, \frac{\lambda_{i'}}{\lambda_i} \exp(-\beta\,\Delta U(s^N))\right] \sim {\rm e}^{\beta\,\Delta\mu} {\rm e}^{-\beta\,\Delta U(s^N)}, \tag{4}$$

where

$$\Delta\mu = \mu_i\,\Delta N_i + \mu_j\,\Delta N_j + \mu_k\,\Delta N_k + \cdots \tag{5}$$

$\Delta U(s^N)$ denotes the change in potential energy due to the identity ($i \rightarrow i'$) flip. For the SiGeC system $\Delta\mu$ would be equal to $\mu_{\rm Si}\,\Delta N_{\rm Si} + \mu_{\rm Ge}\,\Delta N_{\rm Ge} + \mu_{\rm C}\,\Delta N_{\rm C}$. The identity switches can be viewed as Ising-type flips which incorporate the elastic degrees of freedom (effects of strain) explicitly. Equation (4) shows that the system compositions are dictated by the imposed chemical potential differences and by the potential energy changes. In the latter, chemical bond preference plays a significant role. To maximize $P_{\rm acc}^{\rm iden}$ it is necessary that the attempted flips are considerably less in number than the attempted random displacements, and always followed by volume changes, so that all degrees of freedom in the system are sufficiently relaxed.

For the bare Ge/Si case, we work with a fixed system composition, i.e., we assume that a given amount of Ge atoms is deposited on Si(100) and this material forms the WL and the island. In order to equilibrate the system under these conditions, the SGC ensemble is simplified by removing the chemical potential terms in equations (1), (4), since there is no dependence on $\Delta\mu$. This is equivalent to using the (N, P, T) ensemble which, however, still includes identity flips but in the form of *mutual particle interchanges* (e.g. from Si to Ge at a certain site and *vice versa* at another site), so that the composition is kept constant. We consider two possible types of switching move. These are visualized in figure 1.

In the first type, the two atoms are chosen randomly. In the second type, which is the limiting case of the first type, we constrain the two atoms to be nearest neighbours. Obviously, equilibration is reached faster using moves of the first type, because diffusion of atoms at large distances is readily modelled. On the other hand, moves of the second type are more realistic representations of a diffusion event, but need a considerably larger number of moves to diffuse an atom at large distances. Thus an implicit barrier for diffusion at large distances is built in

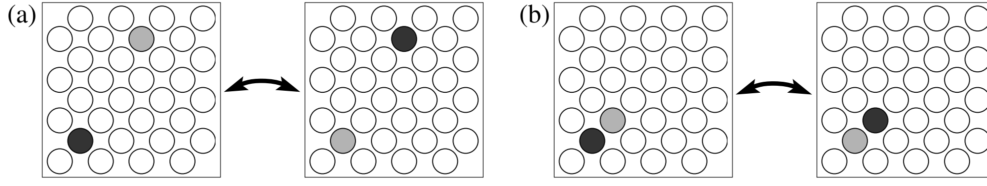

Figure 1. Two different types of switching move: (a) two distant random atoms and (b) two nearest neighbours exchange identities.

with moves of this type. By considering both types, we can test the consistency of the MC equilibration, since at the ergodic limit they ought to lead to similar island compositions. Note that we have no explicit barriers (activation energies) in the switching (exchange) moves of either type, besides the implicit barriers associated with overcoming the small size mismatch. We are currently working on the inclusion of such exchange barriers in the algorithm.

Equilibration within the SGC ensemble is straightforward in systems where the atomic size mismatch among the constituents is small, as in the Ge/Si case. However, semiconductor alloys containing carbon represent a challenging case since the atomic size mismatch in now huge. A carbon atom incorporated substitutionally into the Si or SiGe lattice produces severely strained bonds in the neighbourhood of the insertion, so that very few attempted MC flips involving formation or elimination of a C site, or mutual interchange of C with either Si or Ge, would be accepted, and equilibration is impossible to achieve.

To overcome the large formation energies and diffusion barriers associated with C incorporation, the author devised a modification of the SGCMC algorithm which introduces appropriate relaxations of first-nearest-neighbour (nn) atoms to accompany each attempted move [24–26] (see figure 2). This makes the flips less costly since the 'exchange' barriers are effectively reduced. With this modification the change in the potential energy of the alloy now becomes a sum of three terms:

$$\Delta U(s^N) = \Delta U_{\rm displ}(s^N \to s'^N) + \Delta U_{\rm flip}(s^N) + \Delta U_{\rm relax}(s^N \to s'^N). \tag{6}$$

The first term is the change due to random displacements, the second is due to flips (alterations in chemical bonding), and the third is due to the accompanying relaxations. The last two terms substitute now for $\Delta U(s^N)$ in equation (4). The combined effect of these two terms is expressed as

$$\Delta U(s^N) = E_{\rm cluster}\left(i \to i', \sum_{k=1}^{nn}\sum_{j=1}^{3} \Delta s_k^j(r_{0k}^j)\right) - E_{\rm cluster}^0. \tag{7}$$

The energy is actually estimated over the cluster of atoms affected by the move and the relaxations, instead of over the whole system, before and after the move. The capability for doing this stems from the fact that in the Tersoff potential, as well as in other empirical potentials, e.g. the Stillinger–Weber potential [29], we can decompose the total energy of the system into atomic contributions, and so only the energies of atoms affected by the moves have to be recalculated. This saves an enormous amount of computational time. Each nearest neighbour is relaxed away or towards the central atom (which changes identity from i to i' and is labelled 0) in the bond direction $\vec{r}_{0k}$. This means that every scaled coordinate s^j is altered according to the scheme

$$\Delta s_k^j(r_{0k}^j) = A_{\rm bond} r_{0k}^j, \tag{8}$$

$$A_{\rm bond} = (b_{0k}[i'(0), i(k)] - |\vec{r}_{0k}|)\chi_{\rm rel}/|\vec{r}_{0k}|, \tag{9}$$

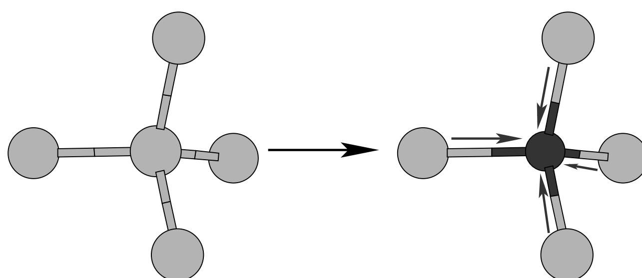

Figure 2. An identity switch of a site from being Si to being C, or *vice versa*, produces strained bonds. In order to make the flips less costly, appropriate relaxations of first-nearest-neighbour atoms are introduced.

where b_{0k} is the bulk equilibrium bond length among atoms 0 (after the flip) and k. The relaxation parameter $\chi_{\rm rel}$, ranging from 0.0 to 1.0, decides how large the relaxation (expressed by $A_{\rm bond}$) should be. We find that intermediate values of $\chi_{\rm rel}$ have the best effect. For values approaching unity, i.e., when the bond relaxes to its ideal bulk value, the success rate drops (but still remains higher than for $\chi_{\rm rel} = 0.0$) due to straining of the back-bonds in the neighbouring atoms.

2.3. Energetics and the structural model

In order to model the interactions and make the simulations tractable, we use the well-established interatomic potentials of Tersoff for multicomponent systems [30]. The potentials were extended by the author to treat the ternary SiGeC system [24], and have been used with success in similar contexts [24, 26]. In particular, bonding and strain fields induced by the surface reconstruction are accurately described, and various predictions made about C interactions and stress compensation are verified experimentally.

When modelling the bare Ge/Si dot case, we start with simulational cells consisting of coherent pure Ge islands. We restrict the discussion to islands having pyramidal shape with a square base and {105} facets, on top of a WL of Ge and a Si substrate in the (100) orientation (Stranski–Krastanov growth mode). The top layer of the WL and the dot facets are reconstructed in the usual 2×1 dimer configuration. The base of the dots is oriented at an angle of 45° with respect to the dimer rows of the WL [31]. The width of the WL is fixed at three monolayers (ML) [31]. The substrate contains 10 ML (the bottom layer is fixed, and identity switches occur down to 8 ML). Due to the limited depth of the Si substrate, the epitaxial strain is imposed by constraining the cells to laterally the Si lattice dimensions. Still, the atoms are free to relax in-plane by moving to their lowest-energy positions under the influence of epitaxial strain. Both lattice and atomic relaxations occur vertically. Periodic boundary conditions are imposed in the lateral directions. The size of the dots varies, the largest one having a base width of 141 Å. The aspect ratio (height over base width, $h/a \sim 0.1$) and the contact angle ($\sim$11°) are close to the experimental values.

One might consider as a limitation of the present approach the neglect of intermixing during growth, since we model interdiffusion once Ge islands have been already nucleated. However, this approach is consistent with experimental evidence [13, 14] that small pyramidal islands, such as those simulated here, *alloy only after they have existed for some time after nucleating* at medium growth temperatures (450–600 °C). More recent work by the same group showed [15] that even at elevated temperatures (700 °C) *pure* Ge islands can be grown,

prior to Si interdiffusion, by raising the deposition rate. Our approach is also consistent with a wide class of post-growth annealing experiments reporting thermally activated intermixing. Experiments of this kind indicate a quasi-equilibrium nature of the process. Other situations that are relevant to this approach include intermixing after the embedding or capping of dots with the host material.

But for the sake of discussion, let us assume that significant intermixing occurs during growth, especially at high temperatures. I argue here that this makes no difference because, as I pointed out above, there is continuously bulk diffusion within the growing island at such temperatures, driving the system into quasi-equilibrium. This means that the composition profile during growth is not frozen as further material is deposited, but it is constantly reorganized until the completion of the island occurs. Therefore, no matter whether we consider diffusion during the various stages of growth or at the end, we are talking about a near-equilibrium composition profile. Of course, at present, we can only speculate about this. We are currently examining the issue of intermixing as the island grows.

I would also like to comment on the possibility for significant intermixing at the starting point of growth. Obviously, this requires an already heavily alloyed WL. This reasoning is counter-intuitive: if the strains and the elastic energy in the wetting layer due to the mismatch were significantly reduced through extensive intermixing, the primary driving force for islanding would be dramatically weakened, and of course the thickness of the alloyed WL would be considerably greater than what is actually measured. In such a case, mainly kinetic factors would be responsible for islanding. This exaggerates the role of kinetic processes. It is thus likely that at first strain is mostly relieved by three-dimensional growth (islanding) and at a second stage by intermixing.

When simulating the C-induced dots, we try to model the experimental conditions as much as possible. So, we first 'predeposit' C atoms in the Si(100) surface by the incorporation process described above, at various sub-monolayer coverages and at 900 K. The Si substrate in our simulational cell contains 9 ML 200 Å $\times$ 200 Å wide. The bottom layer is kept fixed throughout the simulation. The cell is constrained to have laterally the Si lattice dimensions, with relaxation occurring vertically. Periodic boundary conditions are imposed in the lateral directions.

It is now well established that C induces the $c(4\times4)$ reconstruction of the surface, although its structure is still a matter of debate [32–34]. At low coverages, the surface is partly covered with the $c(4\times4)$ configurations involving C atoms, while the rest retains the (2×1) symmetry. It has been shown by the experimental work of Leifeld *et al* [35] that Ge dots nucleate on such C-free areas. The theoretical argument to support this originates from a previous work of the author, who unravelled a repulsive interaction between Ge and C atoms in the Si lattice [24]. To conform with this experimental observation, we do not allow incorporation of C in the central portion of the surface in our simulational cell, producing thus a C-free area. In the C-containing region, the dominant structures are Si–C dimers on the terrace and C atoms in the third and fourth sub-surface layers, at sites below the surface dimers. These are believed to be the main configurations in the $c(4\times4)$ reconstruction at low C contents [33, 34]. To investigate the effect of the amount of C predeposited, we generate cells with 0.16 and 0.36 ML C coverage by varying the C chemical potential.

In the second stage, we form a coherent pure Ge island on top of the C-free area. The dot has a pyramidal shape and orientation as in the bare case, and a base width of $\sim$92 Å. Typically, C-induced dots seen in experiment have similar dimensions. The amount of Ge in the cell is equivalent to $\sim$0.5 ML. With such Ge coverage, the model simulates islands produced by experiment at low substrate temperatures ($\sim$625 K), at which no Ge wetting layer is formed on the terrace [35] (Volmer–Weber mode).

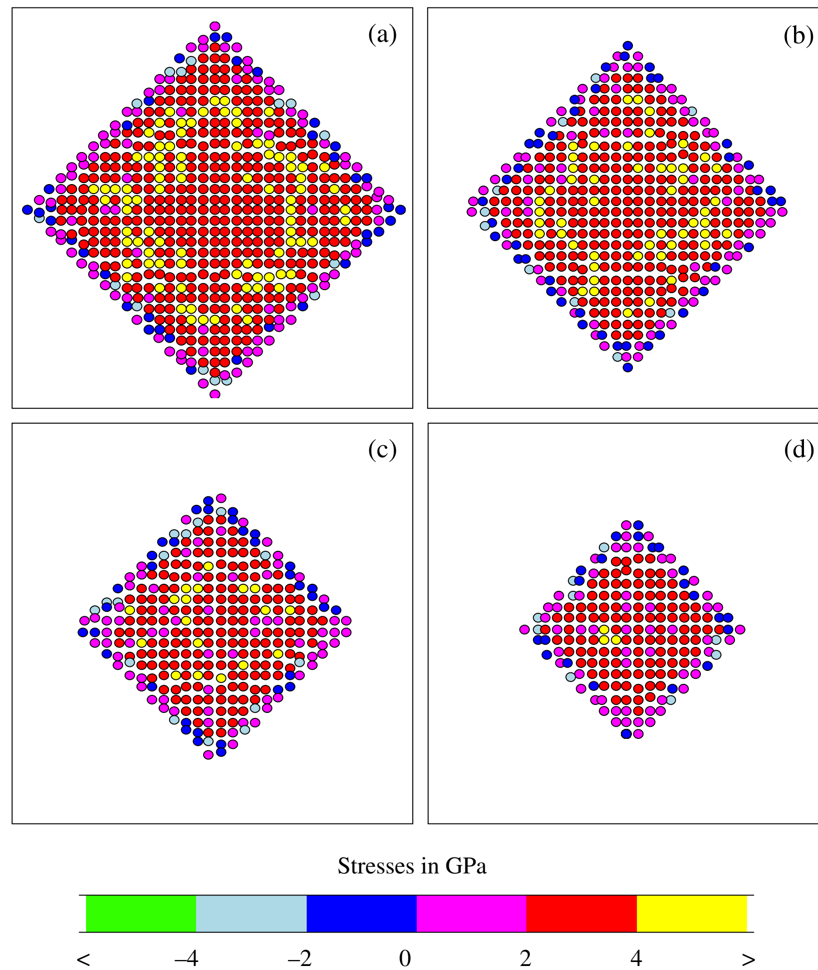

Figure 3. Atomic sites coloured according to their local stress. (a) Base, (b) second, (c) third and (d) fourth dot layer.

3. Results and discussion

3.1. Bare Ge/Si(100)

3.1.1. Stress field. We begin with the analysis of the stress field in the pure Ge islands, since this clarifies and determines the details of the strain-driven intermixing to be discussed below. The stress pattern is probed using the concept of *atomic level stresses* [36]. The local stress can be viewed as an atomic hydrostatic compression (tension), defined by $\sigma_i = -\mathrm{d}E_i/\mathrm{d}\ln V \sim p\Omega_i$, where E_i is the energy of atom i (as obtained by decomposition of the total energy into atomic contributions), and V is the volume. Dividing by the appropriate atomic volume Ω_i converts into units of pressure p. Due to our definition of local stresses, positive (negative) sign indicates compressive (tensile) stress. Summing up the σ_i over a group of atoms in the system (such as over a ML or over the whole island) yields the average stress over the specific configuration.

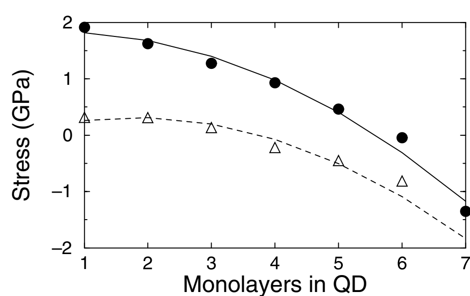

Figure 4. Stress per layer in the QD before (full symbols) and after (open symbols) intermixing.

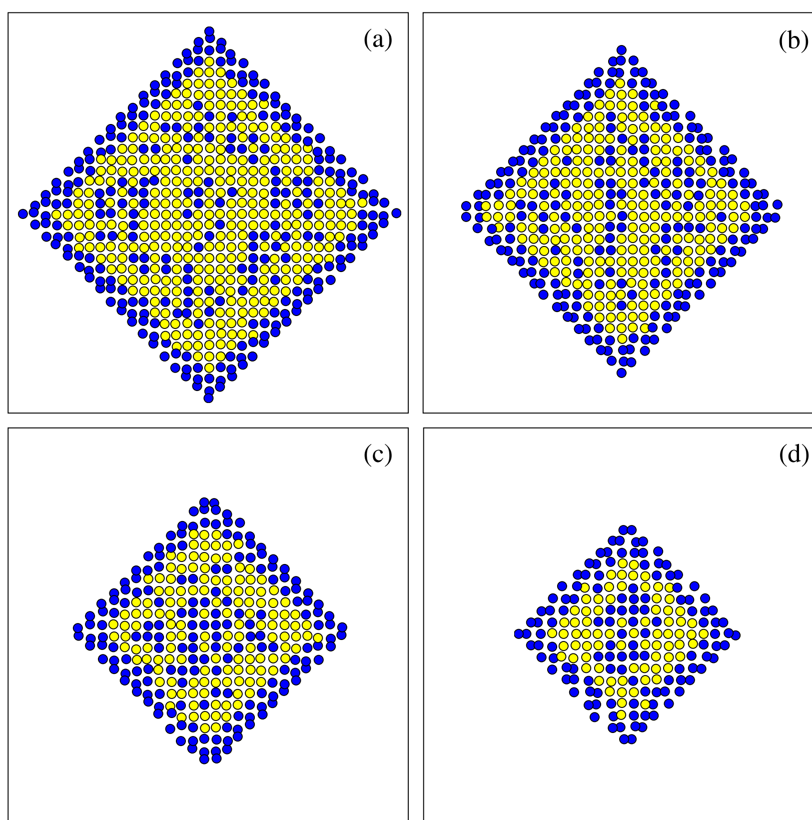

Figure 5. Atomic sites coloured according to their average occupancy. Yellow spheres show Si atoms; blue spheres denote Ge atoms. (a) Base, (b) second, (c) third and (d) fourth dot layer.

The application of this site-by-site analysis is demonstrated in figure 3 for selected layers near the bottom of an island with a base width of 92 Å. The atoms are coloured according to their local stress at 800 K. Three interesting features are revealed in these graphs:

(i) The stresses are overwhelmingly compressive in each layer, especially in the base layer, but compression fades as we move upwards to the top. Only atoms near and around the periphery have neutral or slightly tensile stress. This is because stresses at the facets are tensile due to the dimer reconstruction.

(ii) The overall distribution of stress in the island is inhomogeneous.

(iii) An outstanding feature of marked inhomogeneity is revealed by the ring of highly compressed atoms, formed around the centre of each layer (it is more pronounced in the base layer) and as we approach the edges. It indicates that atoms near the periphery and at the centre are able to relax some excessive stress, leaving the atoms in the ring overcompressed. The ring features fade as we move upwards.

Earlier works [2, 3, 7, 8] have pointed out the accumulation of stress and strain energy in the bottom of pyramidal islands, but not such subtle variations as the local overconcentration of stress within a ring in the bottom layers.

Figure 4 gives a more quantitative picture of the stress conditions in the island. Each full symbol denotes the average stress in a given layer. The solid curve portrays the variation as we move from the base of the island (the layer numbered 1) to the top. A non-linear decrease of compression takes place. Stress near the top varies (is released) more rapidly. The average stress over the whole island $\sigma_{\mathrm{QD}}^{\mathrm{bef}}$ is 1.4 GPa/atom. This shows that despite the three-dimensional formation and the accompanying outward atomic relaxations, the compressive stress in the dot is still substantial.

A similar analysis is carried for the WL. The average stress $\sigma_{\mathrm{WL}}^{\mathrm{bef}}$ is 2.2 GPa/atom, so despite the island formation on top, the WL also remains substantially compressed. Most of the compression is stored in areas below the dot, especially around the periphery. Similar findings were reported by other researchers as well [9]. The most compressed layer is the middle one because the 2×1 reconstruction at the terrace around the island induces large compressive stresses in the layer below [36]. At the top surface layer, the terrace is practically free of stress, while the area below the dot is heavily compressed.

Stress conditions change dramatically when we allow atom-identity flips, and thus permit interdiffusion of species between the three components of the system (QD, WL, and substrate). Let us analyse the layer-by-layer average stresses shown in figure 4 (open symbols, dashed curves). A remarkable reduction of compressive stress takes place in the QD, especially near its base. Now, the average stress in the island $\sigma_{\mathrm{QD}}^{\mathrm{aft}}$ is 0.1 GPa/atom, nearly compensated. This shows clearly that the dominant factor driving segregation in the island is stress relaxation, much more powerful in this case than the intrinsic tendency of the Si–Ge system to randomly mix. Equally important is the relaxation of stress in the WL, where the average stress $\sigma_{\mathrm{WL}}^{\mathrm{aft}}$ is now 0.9 GPa/atom.

3.1.2. Composition profiles. The composition profiles in the islands can be mapped by extracting the local compositions, which are indicated by the average site occupancies. These are calculated using the switching–exchange moves depicted in figure 1. At the ergodic limit of many thousands of attempted flips per site, both flip modes lead essentially to the same average occupancies. Once this is completed, the *average* occupancies are compared to the respective *random* ones, which would be the result of a random distribution of atoms on the lattice sites, in order to allow us to infer the average identity of each site.

Figure 5 illustrates the atomic sites in selected layers near the bottom of the island, coloured according to their average identity. A highly non-uniform pattern arises. The periphery is clearly decorated with Ge atoms. In the interior, the centre of each layer is rather rich in Ge, especially as we move up. Si atoms are mostly found in and around the overcompressed ring of sites, shown in the stress pattern of figure 3; this is because sites under compression tend to be occupied by the smaller species in the system [36]. Thus, local stress conditions determine to a large degree the inhomogeneous features of the composition profile. The other important factor, that competes with the stress factor in shaping the profile, is the lower surface energy of Ge.

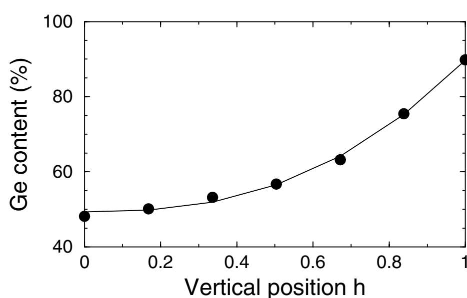

Figure 6. The vertical variation of the Ge content in the intermixed island.

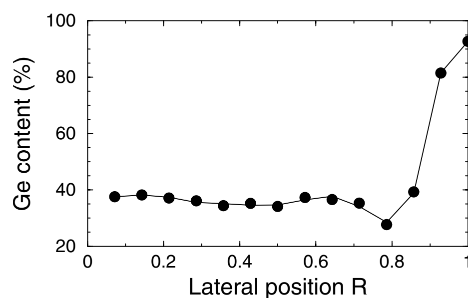

Figure 7. The lateral variation of the Ge content in the base layer.

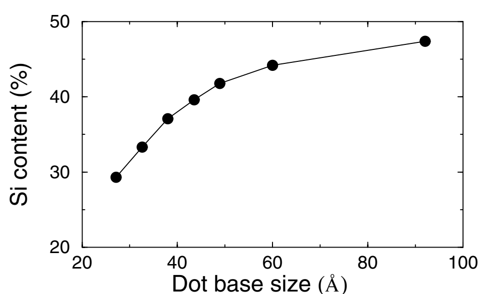

Figure 8. The size dependence (at 800 K) of the Si content in pyramidal islands.

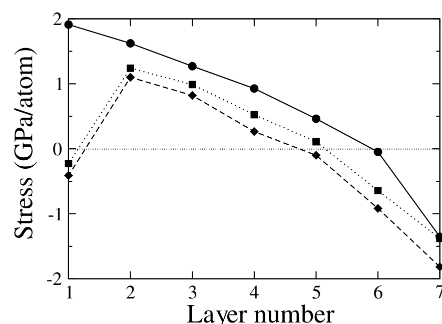

Figure 9. Variation of average stress layer by layer in the dot at 625 K. The layer numbered 1 denotes the base in the dot. Positive (negative) sign indicates compressive (tensile) stress.

This factor is particularly strong in the periphery and at the faceted edges. If we had to describe in a sentence the 3D character of the profile, we would say that *Ge forms the core of the pyramid and covers the facets, while Si forms a hollow cone bounded by the core and the outer Ge*. However, some caution is needed when comparing the outer Ge profile with experimental results from CVD experiments. In the latter, hydrogen is expected to have a significant surfactant action, and it is very likely that the facet surfaces will turn out to be less rich in Ge.

A quantitative description of the overall composition profiles in the island can be easily extracted from this analysis. The vertical variation of Ge content as a function of the normalized island height h (measured from the base) is shown in figure 6. It is extracted by calculating an average value within each layer. It is near parabolic and is very well fitted with the power law function, $x_{\mathrm{Ge}} = a_0 + a_1 h^{a_2}$, with $a_0 \simeq 50$, $a_1 \simeq 40$, and $a_2 = 2.5$. Thus, the Ge content is slowly varying in the bottom and rapidly varying when approaching the top of the island. We checked that this simple behaviour is valid in all cases studied, with the exponent lying in the range of values 2.5 ± 0.2. Note that the form of the variation is consistent with the form of the variation of stresses in the pure island; i.e., the larger the compression the higher the Si content in the specific layer.

Liao *et al* [19] used energy dispersive x-ray spectrometry to extract the vertical variation of the relative Si/Ge ratio in dislocated islands. They found this ratio to be higher closer to the substrate, in agreement with our results, but its variation is opposite to ours: the Ge fraction increases rapidly in the bottom and remains nearly constant at the top. Possible sources of

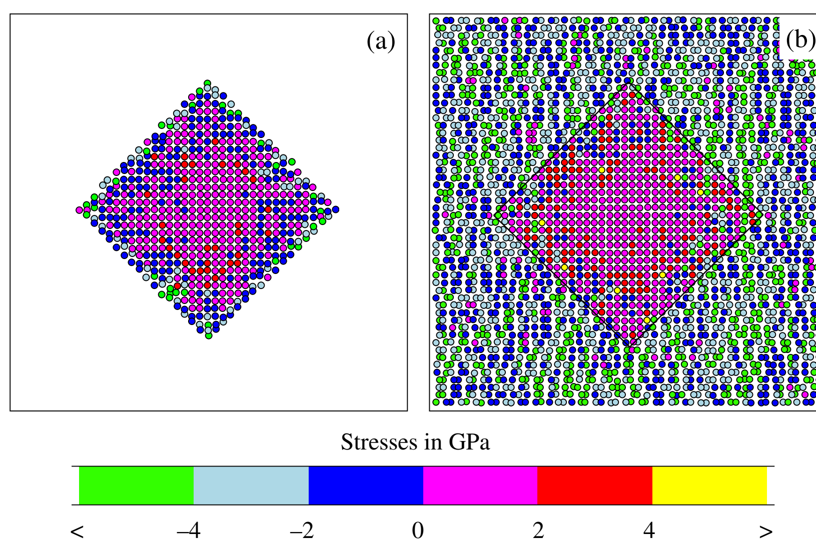

Figure 10. Atomic sites coloured according to their local stress. (a) Base dot layer. (b) Top substrate layer. Solid lines (guide to the eye) enclose the area below the island.

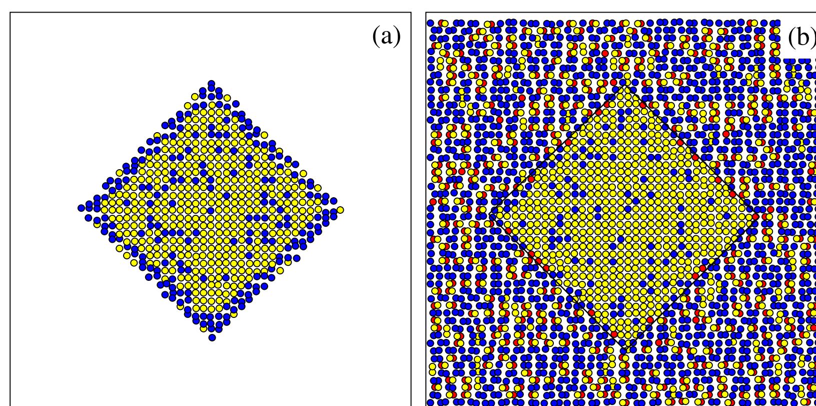

Figure 11. Atomic sites coloured according to their average occupancy. Yellow spheres show Si atoms, blue spheres denote Ge atoms, and red spheres show C atoms. (a) Base dot layer. (b) Top substrate layer. Solid lines (guide to the eye) enclose the area below the island.

this discrepancy might be the neglect in the experimental analysis of the lateral variations of composition, which by necessity affect the outcome for the vertical variations. A more recent work by Schülli *et al* [20] using anomalous x-ray diffraction also found a rapid variation of Ge at the bottom, with an abrupt jump from $\sim$10 % to $\sim$80 %, but again lateral variations were neglected. Also, it is hard to explain why there is such an abrupt jump in Ge content when the evolution of the in-plane lattice parameter relaxation in the islands, as reported by the same experiment, has a closely linear behaviour.

The lateral variation is constructed by drawing concentric shells of square shape, starting from the centre of the layer and moving outwards to the edges. Within each shell an average Ge content is calculated from the site occupancies, and is plotted versus the normalized radius R measured from the centre. This is drawn for the base-layer lateral variation in figure 7.

An accurate fit to the variation is made using higher-order polynomials. Although the polynomial coefficients vary from layer to layer, there is a unique and common composition behaviour in all layers in the dot. The variation is characterized by slight oscillations of the Ge content up to a distance of ∼0.6–0.7, where a deep minimum appears, and then by a steep increase in Ge content on approaching the edges. Thus, the Si content is indeed enhanced within the shells of overcompressed sites near the edges, as observed above from the visual inspection, but not at the boundary, as proposed by Chaparro *et al* [13], because of the lower surface energy of Ge.

An interesting comparison of our inhomogeneous composition profile can be made with the work of Liu *et al* [11] on $In_{0.5}Ga_{0.5}As$ QDs. They found an inhomogeneous profile with an In-rich core having an inverted-triangle shape. The two profiles agree in that the top region of the island is enriched with the larger-misfit component (In in one case, Ge in the other). A striking difference is that our profile shows Ge enriching the regions near the edges, even at the bottom of the dot, while they find the In fraction to decrease from centre to edge and vanish at the bottom region of the island outside the In-rich core. This difference indicates that, beside the chemistry, the lateral variations of stress are dissimilar in the two classes of heteroepitaxial systems.

The average of site occupancies over the whole island yields a Si content of ∼47% at 800 K. The Si content in the WL is 58%. At a higher temperature (∼1150 K), Capellini *et al* [18] found from photoemission measurements that the Si content in Ge/Si epilayers (QD plus WL) rises to 72%. Our result for the epilayer at this temperature is ∼55%. A possible reason for this difference is again the neglect of lateral variations in the modelling used to extract the compositions from the measurements. Better agreement is reached with the work of Zhang *et al* [15] who found a Si content of 56% in dome islands at ∼1000 K. At this temperature our pyramids contain ∼49% of Si. Taking into account that domes probably have somewhat higher Si contents brings theory and experiment into very good agreement. Also, note that the Si content in larger dots, especially domes, is expected to be controlled by diffusion through trenches surrounding the islands. We neglected this feature in the present work dealing with small pyramids. We have recently studied in detail the effect of trenches, and results will be published soon.

It is also interesting to know how the Si content in the dot varies with size. We demonstrate this dependence in figure 8. We observe that the Si content (at 800 K) initially rises sharply with dot size, but it eventually reaches a limiting value that seems to stay close to 50% for larger islands. This means that beyond a critical size the composition remains nearly constant. This result is also in agreement with the recent work of Zhang *et al* [15] who found that the composition appears to be independent of island size.

Concluding this part of the paper, I would like to stress the existence of inhomogeneous composition profiles in the islands, and that this non-uniformity is largely determined by the stress field. Experiments need to take into account the lateral variations. From the theory point of view, we need to consider larger islands in order to confirm the above trends and show that they do not depend on the size. Work towards this goal is in progress.

3.2. C-induced dots

When C enters substitutionally into the Si lattice major strains are generated around the sites of insertion, leading to long-ranged stress fields [37]. In the case of SiGe alloys, C produces an additional effect [24]: it preferentially bounds to Si atoms, and repels the Ge atoms. This is due to the weakness of the Ge–C bond, having a high positive enthalpy of formation (∼2 eV/atom), and to the well-known great strength of the Si–C bond. Thus, in the general case of the ternary

SiGeC system, strain and chemical effects compete with each other in shaping up the structure and the composition profiles.

A striking manifestation of such C-induced interplay is seen in the case of Ge islands formed on a Si(100) surface, which is precovered with a small amount of C. These islands are a special and important class of Si-based nanostructures. They are fabricated by molecular beam epitaxy [32, 35, 38, 39] and attracted interest because they are remarkably small—typical sizes are 10–15 nm in diameter and 1–2 nm in height—and exhibit intense photoluminescence (PL) [39]. The growth of these islands proceeds without the formation of a wetting layer (Volmer–Weber mode), contrary to the islands grown on bare Si(100) which follow the Stranski–Krastanov growth mode. This is attributed to the predeposited C atoms. Their small size reduces the lattice constant of the alloyed Si surface and exaggerates the mismatch with the Ge overlayer. In addition, C atoms modify the surface and interface energetics.

Since C atoms play such a vital role, it is essential to know how they are distributed in the surface region, and especially whether they occupy sites in and below the dots. The interpretation of PL data strongly depends on this information, but the issue is controversial. There have been two different models drawn from experimental work. In the work of Schmidt and Eberl [39], the PL data were interpreted as suggesting that the dots have a gradual composition profile from homogeneous SiGeC below and at the bottom to pure Ge towards their apex. On the other hand, Grützmacher and co-workers [35] interpreted their STM images as suggesting that the dots are free of C, have a gradual composition profile from SiGe at the bottom to Ge at the apex, and are located between C-rich patches. Our simulations offer an answer and resolve this debate. What follows is based on the structural model described in the methodology section.

3.2.1. Stress field. We first analyse the stress state of the initial configuration using the atomic level stresses σ_i, as in the bare case. It comes out from this analysis that, in the presence of C, the stress pattern deviates significantly from the bare Ge/Si case. This is demonstrated in figure 9. It is clear that the overall compressive stress in the dot is significantly reduced under the influence of C, and that this reduction is enhanced as the amount of predeposited C increases. The average stress in the dot $\bar{\sigma}_{\mathrm{QD}}$ for the bare case was shown above to be 1.4 GPa/atom. For 0.16 ML C, $\bar{\sigma}_{\mathrm{QD}} = 0.45$ GPa/atom, while for 0.36 ML C, $\bar{\sigma}_{\mathrm{QD}} = 0.27$ GPa/atom. In the substrate, tensile conditions prevail, especially on the terrace, because the C atoms experience large local tensile stresses. This is partly compensated in the first sub-surface layer where the surface reconstruction induces compressive conditions [36].

The most noticeable change due to C is observed in the bottom layer of the dot. It is found to be under slight tension, contrary to the bare case in which this layer is very compressed. The effect originates from certain Ge atoms which are under excessive tensile stress. To get more insight into this effect, we resort to the site-by-site analysis of the stress pattern. This is illustrated in figure 10 for selected layers of the cell with 0.16 ML C content. It is clearly shown that a large number of Ge atoms in the base layer of the dot are under tension, not only at the periphery but also in regions inside, while the central region is compressed. In the bare case only the peripheral Ge atoms are under tension. We can think of this effect as a 'dragging out' of the exterior regions of the base layer to conform with the contracted surrounding lattice due to C incorporation. The effect considerably weakens in the second layer, not shown, which is mostly under compression (but still lower than in the bare case). On the terrace, tensile stresses dominate around the dot, but the region just below the dot is mostly compressed as in the base dot layer. The first sub-surface layer exhibits regions of tensile stress, especially under the dot. This compensates for the compression above on the terrace and the base layer.

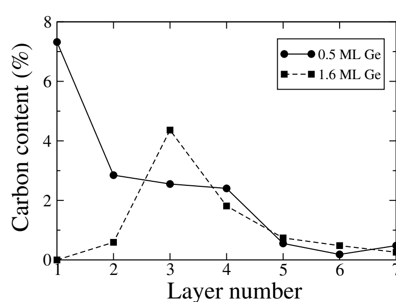

Figure 12. The carbon content in substrate layers. The layer numbered 1 denotes the top layer. The C coverage is 0.36 ML.

3.2.2. Composition profiles. At higher temperatures (∼800 K), intermixing of Ge with C in the Si–C areas, which was initially inhibited due to the Ge–C repulsion, is believed to take place [35]. To address this possibility and obtain the equilibrium distribution of the species appropriate for high temperature, the initial configuration is further relaxed at 800 K by interdiffusion. To model this, we use again the flipping moves of figure 1, complemented with the relaxation moves of figure 2. The associated analysis of the site occupancies, as in the bare case, leads to the average identity of each site.

The application of this analysis to the cell with 0.36 ML C content is shown in figure 11, for selected layers. The atoms are coloured according to their average identity. The outstanding feature revealed in these graphs is the complete absence of carbon from the dot layers (only the base layer is shown). We repeated the simulation for an even higher temperature (1000 K), to increase further the acceptance of flipping moves, and found the same result. We can point out two factors responsible for this:

(a) C has to break Ge–Ge bonds in the dot and form instead Ge–C bonds, which are unstable as mentioned above.
(b) The compressive stress in the dot is better compensated by the segregation of Si than that of C.

The latter would induce tensile conditions. So, Si atoms diffuse into the island, while Ge atoms diffuse out from the interior to wet the terrace due to their low surface energy, mostly forming Ge–Ge dimers and a few Ge–Si dimers. C atoms on the terrace are solely involved in Si–C dimers.

Interestingly, the areas on the terrace and in deeper layers, which are underneath the island base, also remain free of carbon after the redistribution of species. Note that the Ge and Si composition profiles in the island are quite similar to the respective profiles in the bare Ge/Si case (see above). The Ge content is slowly varying in the bottom and rapidly varying when approaching the top of the island (not shown here). Taking all these observations into account, we conclude that there is no evidence for SiGeC alloying in the dot or below, and that our theoretical model is in general consistent with the experimental model of Grützmacher.

It is reported that at higher Ge coverages the C-induced dots show improved PL [39, 40]. We therefore investigated the distribution of species in this important case. We start with a configuration where Ge fully wets the terrace, covering the predeposited C-rich areas surrounding the island, as is done in experiments. This is equivalent to 1.6 ML Ge coverage. Then, the structure is equilibrated and relaxed by intermixing at 800 K. Again, we find that the dot remains free of C. But most importantly, the terrace is also free of C, and the layer below contains a very small amount of it. Instead, C content is maximized in the third layer. This is

clearly demonstrated in figure 12, which compares this case with the C profile for 0.5 ML Ge coverage. Obviously, the Ge–C repulsion forces C into deeper layers. On the other hand, Ge atoms are found to stay on top. We conclude that the relaxed Ge overlayer covers the Si–C geometries.

This has an important consequence. The average of the site occupancies over the whole island yields its Ge content. This comes out to be ∼60%, for 0.36 ML C, compared to ∼50% for the bare case. We interpret this to mean that C atoms in deeper layers act as a trap of Si atoms. This decelerates the diffusion of Si in the dot, and the out-diffusion of Ge, so enhancing the Ge content and providing better confinement conditions. We expect that for 2.5 ML Ge, where the PL signal is at the maximum [40], the enhancement of Ge content in the dot will be even stronger.

4. Conclusions

I reviewed in this paper recent simulational work addressing the issues of stress and composition in bare Ge/Si and C-induced Ge/Si islands. I have, in detail, described the efficient MC algorithms used to achieve quasi-equilibrium between the metastable thermodynamical states characterizing the dots, and I emphasized the physical considerations leading us to adopt such a theory of quasi-equilibrium. For the bare case, it was shown that the stress field and the composition profiles are directly linked. In the case of C-induced Ge dots, we gave firm answers about the composition and stress field and resolved the controversy between experimental studies.

Acknowledgments

The author thanks Ph Sonnet and G Hadjisavvas for setting up and carrying out the simulations. This work was partly supported by the EU RTN programme under Grant No HPRN-CT-1999-00123.

References

[1] Tersoff J and Tromp R M 1993 *Phys. Rev. Lett.* **70** 2782
Tersoff J and LeGoues F K 1994 *Phys. Rev. Lett.* **72** 3570
[2] Barabási A 1997 *Appl. Phys. Lett.* **70** 2565
[3] Kästner M and Voigtländer B 1999 *Phys. Rev. Lett.* **82** 2745
[4] Tersoff J, Teichert C and Lagally M G 1996 *Phys. Rev. Lett.* **76** 1675
[5] Ross F M, Tersoff J and Tromp R M 1998 *Phys. Rev. Lett.* **80** 984
[6] Yu W and Madhukar A 1997 *Phys. Rev. Lett.* **79** 905
[7] Moll N, Scheffler M and Pehlke E 1998 *Phys. Rev.* B **58** 4566
[8] Jesson D E, Chen G, Chen K M and Pennycook S J 1998 *Phys. Rev. Lett.* **80** 5156
[9] Raiteri P, Miglio L, Valentinotti F and Celino M 2002 *Appl. Phys. Lett.* **80** 3736
[10] Tersoff J 1998 *Phys. Rev. Lett.* **81** 3183
[11] Liu N, Tersoff J, Baklenov O, Holmes A L and Shih C K 2000 *Phys. Rev. Lett.* **84** 334
[12] Kirfel O, Müller E, Grützmacher D and Kern K 2003 *Physica* E **16** 602
[13] Chaparro S A, Drucker J, Zhang Y, Chandrasekhar D, McCartney M R and Smith D J 1999 *Phys. Rev. Lett.* **83** 1199
[14] Chaparro S A, Zhang Y, Drucker J, Chandrasekhar D and Smith D J 2000 *J. Appl. Phys.* **87** 2245
[15] Zhang Y, Floyd M, Driver K P, Drucker J, Crozier P A and Smith D J 2002 *Appl. Phys. Lett.* **80** 3623
[16] Boscherini F, Capellini G, Di Gaspare L, Rosei F, Motta N and Mobilio S 2000 *Appl. Phys. Lett.* **76** 682
[17] Henstrom W L, Liu C, Gibson J M, Kamins T I and Williams R S 2000 *Appl. Phys. Lett.* **77** 1623
[18] Capellini G, De Seta M and Evangelisti F 2001 *Appl. Phys. Lett.* **78** 303
[19] Liao X Z, Zou J, Cockayne D J H, Jiang Z M, Wang X and Leon R 2000 *Appl. Phys. Lett.* **77** 1304

[20] Schülli T U, Stangl J, Zhong Z, Lechner R T, Sztucki M, Metzger T H and Bauer G 2003 *Phys. Rev. Lett.* **90** 066105
[21] Denker U, Stoffel M and Schmidt O G 2003 *Phys. Rev. Lett.* **90** 196102
[22] Sonnet Ph and Kelires P C 2002 *Phys. Rev.* B **66** 205307
[23] Hadjisavvas G, Sonnet Ph and Kelires P C 2003 *Phys. Rev.* B **67** 241302(R)
[24] Kelires P C 1995 *Phys. Rev. Lett.* **75** 1114
[25] Kelires P C 1998 *Int. J. Mod. Phys.* C **9** 357
[26] Kelires P C 1998 *Surf. Sci.* **L418** 62
[27] Frenkel D 1991 *Computer Simulations in Materials Science* (*NATO ASI Ser. E* vol 205) ed M Mayer and V Pontikis (Dordrecht: Kluwer–Academic) p 85
[28] Metropolis N, Rosenbluth A W, Rosenbluth M N, Teller A H and Teller E 1953 *J. Chem. Phys.* **21** 1087
[29] Stillinger F and Weber T 1985 *Phys. Rev.* B **31** 5262
[30] Tersoff J 1989 *Phys. Rev.* B **39** 5566
[31] Mo Y W, Savage D E, Swartzentruber B S and Lagally M G 1990 *Phys. Rev. Lett.* **65** 1020
[32] Leifeld O, Grützmacher D, Müller B, Kern K, Kaxiras E and Kelires P C 1999 *Phys. Rev. Lett.* **82** 972
[33] Remediakis I N, Kaxiras E and Kelires P C 2001 *Phys. Rev. Lett.* **86** 4556
[34] Sonnet Ph, Stauffer L, Selloni A, De Vita A, Car R, Simon L, Stoffel M and Kubler L 2000 *Phys. Rev.* B **62** 6881
[35] Leifeld O, Beyer A, Grützmacher D and Kern K 2002 *Phys. Rev.* B **66** 125312
[36] Kelires P C and Tersoff J 1989 *Phys. Rev. Lett.* **63** 1164
[37] Kelires P C and Kaxiras E 1997 *Phys. Rev. Lett.* **78** 3479
[38] Schmidt O G, Lange C, Eberl K, Kienzle O and Ernst F 1997 *Appl. Phys. Lett.* **71** 2340
[39] Schmidt O G and Eberl K 1998 *Appl. Phys. Lett.* **73** 2790
[40] Beyer A, Leifeld O, Stutz S, Müller E and Grützmacher D 2000 *Nanotechnology* **11** 298